Interaction of heparin with internally quenched fluorogenic peptides derived from heparin-binding consensus sequences, kallistatin and anti-thrombin III

Daniel C. PIMENTA*, Iseli L. NANTES†, Eduardo S. DE SOUZA‡, Bernard Le BONNIEC§, Amando S. ITO‡, Ivarne L. S. TERSARIOL†, Vitor OLIVEIRA‖, Maria A. JULIANO‖ and Luiz JULIANO‖[1]

*Centro de Toxinologia Aplicada, CAT/CEPID, Av. Vital Brasil, 1500, São Paulo SP-05503-900, Brazil, †Centro Interdisciplinar de Investigação Bioquímica (CIIB), UMC, Avenida Cândido Xavier de Almeida Souza, 200, Mogi das Cruzes-SP, 08780-911, Brazil, ‡Departamento de Física e Matemática, FFCLRP, Universidade de São Paulo, Av. Bandeirantes 3900, Ribeirão Preto, SP 14040-901, Brazil, §INSERM, U428, Université Paris V, Faculté de Pharmacie, 4 Avenue de l'Observatoire, 75270 Paris, cedex 06, France, and ‖Universidade Federal de São Paulo, Escola Paulista de Medicina, Departmento de Biofísica, Rua Três de Maio, 100, São Paulo 04044-020, Brazil

Internally quenched fluorogenic (IQF) peptides bearing the fluorescence donor/acceptor pair *o*-aminobenzoic acid (Abz)/*N*-(2,4-dinitrophenyl)ethylenediamine (EDDnp) at N- and C-terminal ends were synthesized containing heparin-binding sites from the human serpins kallistatin and antithrombin, as well as consensus heparin-binding sequences (Cardin clusters). The dissociation constant (K_d), as well as the stoichiometry for the heparin–peptide complexes, was determined directly by measuring the decrease in fluorescence of the peptide solution. Experimental procedures were as sensitive as those used to follow the fluorescence change of tryptophan in heparin-binding proteins. The conformation of the peptides and the heparin–peptide complexes were obtained from measurements of time-resolved fluorescence decay and CD spectra. Kallistatin (Arg^{300}–Pro^{319})-derived peptide (HC2) and one derived from antithrombin III helix D [(AT3D), corresponding to Ser^{112}–Lys^{139}], which are the heparin-binding sites in these serpins, showed significant affinity for 4500 Da heparin, for which K_d values were 17 nM and 100 nM respectively. The CD spectra of the heparin–HC2 peptide complex did not show any significant α-helix content, different from the situation with peptide AT3D, for which complex-formation with heparin resulted in 24 % α-helix content. The end-to-end distance distribution and the time-resolved fluorescence-decay measurements agree with the CD spectra and K_d values. The synthetic α-methyl glycoside pentasaccharide AGA*IA$_M$ (where A represents N,6-O-sulphated α-D-glucosamine; G, β-D-glucuronic acid; A*, N,3,6-O-sulphated α-D-glucosamine; I, 2-O-sulphated α-L-iduronic acid; and A$_M$, α-methyl glycoside of A) also binds to AT3D and other consensus heparin-binding sequences, although with lower affinity. The interaction of IQF peptides with 4500 Da heparin was displaced by protamine. In conclusion, IQF peptides containing Abz/EDDnp as the donor/acceptor fluorescence pair are very promising tools for structure–activity relationship studies on heparin–peptide complexes, as well as for the development of new peptides as heparin reversal-effect compounds.

Key words: binding assay, glycosaminoglycan, kallikrein, time-resolved fluorescence.

INTRODUCTION

Glycosaminoglycans (GAGs) bind to a large number of proteins, taking part in a myriad of biological functions, such as the modulation of proteolytic enzymes and their inhibitors, the regulation of cell growth and the assembly of extracellular matrix [1]. Antithrombin requires activation by heparin in order to inhibit thrombin and factor X_a, which are their main targets, and the mechanisms of inhibition depend on the protease [2–7]. Unlike most of the serpins that have their protease-inhibition activity accelerated by heparin, kallistatin, which is a specific serpin that inhibits human tissue kallikrein, has heparin as a suppressor of its inhibitory activity [8]. Moreover, GAGs have been demonstrated to modulate the reactivity and resistance to pH denaturation of cysteine proteases, such as papain [9] and cathepsin B [10]. The regulatory role of GAGs in cell adhesion, cell motility, cell proliferation and tissue morphogenesis is due to their ability to bind to laminin [11,12], chemokines [13] and growth factors [14] (for a general review, see [15]).

GAGs bind to either peptides or protein domains that exhibit certain preferred conformations [16,17], or induce conformational changes upon its binding [6,18]. Heparin is often used as a model to examine the effects of GAGs on the structure of proteins [19,20] and peptides [21]. Heparin interaction with proteins has usually been monitored by fluorescence change of tryptophan [22], depending on this amino acid being present in the protein and also on whether heparin changes its environment upon binding. The interaction of heparin with tryptophan-containing peptides is not expected to cause significant variation in the amino acid environment and, consequently, no change would be detected in its fluorescence signal. Therefore heparin binding to peptides has been assayed through the use of fluorescence-anisotropy changes [18]: the binding of peptides to radiolabelled or biotinylated heparin, whose complexes are detected by a retarded migration in comparison with heparin on affinity co-electrophoresis gels [21], or by competition with a protein that binds heparin [8,23].

The design of peptides aimed to neutralize the effects of heparin as an alternative to protamine has been tried because of the side effects of this mixture of arginine-rich basic peptides from fish-sperm nuclei [21,24]. Extensive studies on the structure–activity relationship of the interaction of different forms of heparins with peptides and the effects of physical or chemical agents on this interaction have limitations owing to the absence of a sensitive and

Abbreviations used: Abz, *o*-aminobenzoic acid; EDDnp, *N*-(2,4-dinitrophenyl)ethylenediamine; GAG, glycosaminoglycan; IQF, internally quenched fluorogenic; MALDI-TOF, matrix-assisted laser desorption–time-of-flight.

[1] To whom correspondence should be addressed (e-mail juliano.biof@epm.br).

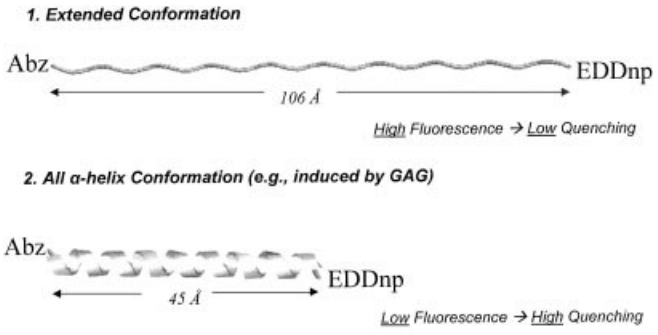

Figure 1 Comparison between two possible conformations of peptide RKK-4 (Table 1), determined by molecular modeling using HyperChem software (Hypercube Inc., Gainesville, FL, U.S.A., http://www.hyper.com)

Shown is the drastic structural change upon heparin binding, as suggested by the CD signal: the end-to-end distance is reduced by more than 50%, leading to an increase in the efficiency of the fluorescence quenching.

easy-to-handle method for the determination of the dissociation constant, K_d. Internally quenched fluorogenic (IQF) peptides have been used as very efficient peptide substrates for proteolytic enzymes [25–27]. The efficiency of the fluorescence quenching is highly dependent on the distance separating the fluorescence donor and the fluorescence quencher groups [28]. Therefore there are limits for the size of the peptides, above which the quenching of the fluorescence is ineffective and the sequences do not function as IQF peptides. If heparin binds to such peptides, inducing preferred structures and leading to a shorter end-to-end distances when compared with their random conformation in solution, a decrease in the fluorescence signal would occur, which is a consequence of the diminishing of the distance separating the fluorescence donor and acceptor groups (Figure 1). In the present study, we have explored this possibility, synthesizing previously described peptides [21] on the basis of the heparin-binding consensus sequences XBBXBX and XBBBXXBX (where 'X' represents hydropathic or uncharged amino acids, and 'B' represents basic amino acids) containing the fluorescent probe *o*-aminobenzoic acid (Abz; the donor) and the quencher group Gln-[*N*-(2,4-dinitrophenyl)ethylenediamine (EDDnp)] (the acceptor) at the N- and C-terminal ends respectively. These motifs were determined by Cardin and Weintraub [29] on the basis of an extensive survey of amino acid sequences present on known heparin-binding proteins. We have also synthesized IQF peptides derived from the heparin-binding sites of antithrombin III and kallistatin and assayed the effect of low-molecular-mass heparin (4500 Da, modal mass) on the fluorescence of all obtained peptides. In the present study, IQF peptides derived from the reactive centre loops of kallistatin and α_1-antichymotrypsin were examined, since heparin is known to impair the inhibitory activities of these two serpins over their target serine proteases [8,30]. In addition, we have also examined the interaction of IQF peptides derived from the heparin-binding sites of antithrombin III and two model heparin-binding peptide with synthetic α-methyl glycoside pentasaccharide AGA*IA$_M$ (where A represents N,6-O-sulphated α-D-glucosamine; G, β-D-glucuronic acid; A*, N,3,6-O-sulphated α-D-glucosamine; I, 2-O-sulphated α-L-iduronic acid; and A$_M$, α-methyl glycoside of A). The dissociation constants (K_d values) for the interaction of IQF peptides with heparin or the pentasaccharide were determined on the basis of the decrease in the fluorescence signal caused by the addition of heparin or the pentasaccharide over a buffered range of IQF peptide solutions. Furthermore, we have examined the conformation of the IQF peptides in their free form and complexed with heparin by using CD spectroscopy, as well as by time-resolved fluorescence.

MATERIALS AND METHODS

Reagents

Low-molecular-mass heparin (4500 Da, modal mass) was purchased from Aventis (Parsippany, NJ, U.S.A.). The pentasaccharide AGA*IA$_M$ was synthesized and provided by Sanofi Recherche (Toulouse, France). The concentration of the oligosaccharides was determined by stoichiometric titrations with antithrombin of known concentration [22]. Protamine and all chemicals used were from Sigma–Aldrich (St. Louis, MO, U.S.A.) or from Calbiochem (San Diego, CA, U.S.A.).

Synthetic substrates

All the IQF peptides contained EDDnp attached to glutamine, a necessary result of the solid-phase peptide synthesis strategy employed, as described previously [31]. An automated bench-top simultaneous multiple solid-phase peptide synthesizer (PSSM 8 system, from Shimadzu) was used for the solid-phase synthesis of all the peptides using the fluoren-9-ylmethoxycarbonyl ('Fmoc') procedure. The final deprotected peptides were purified by binary semi-preparative HPLC using an Econosil C-18 column (10 μm, 22.5 mm × 250 mm) and solvents A [trifluoroacetic acid/H_2O (1:1000, v/v)], and B [trifluoroacetic acid/acetonitrile/H_2O (1:900:100, by vol.)]. The column was eluted at a flow rate of 5 ml/min with a 10–60% gradient of solvent B over the course of 30 to 45 min, depending on the sequence. Analytical HPLC was performed using a binary HPLC system from Shimadzu with a SPD-10AV Shimadzu UV–visible light detector and a Shimadzu RF-10AXL fluorescence detector, coupled with an Ultrasphere C-18 column (5 μm, 4.6 mm × 150 mm) that was eluted with solvent systems A and B at a flow rate of 1 ml/min and a 10–80% gradient of B over 20 min. The HPLC column eluates were monitored by their absorbance at 220 nm and by fluorescence emission at 420 nm following excitation at 320 nm. The molecular mass and purity of synthesized peptides were checked by matrix-assisted laser-desorption–time-of-flight (MALDI-TOF) MS (TofSpec-E, Micromass, Manchester, U.K.) and/or peptide sequencing using a protein sequencer PPSQ-23 (Shimadzu Tokyo, Japan).

Heparin binding to IQF peptides

Heparin binding to IQF peptides was measured at 37 °C in 50 mM Tris/HCl buffer, containing 100 mM NaCl and 0.2% (w/v) poly(ethylene glycol) 6000 ('PEG 6000'), pH 7.4, except where different conditions are stated. The fluorescence of the peptide solutions was monitored by measuring the fluorescence at $\lambda_{em} = 420$ nm (20 nm slit) after excitation at $\lambda_{ex} = 320$ nm (10 nm slit) in a Hitachi F-2000 spectrofluorimeter. The 1 cm path-length cuvette containing 2 ml of the buffered peptide solution was placed in a thermostatically controlled cell compartment under constant magnetic stirring in the spectrofluorimeter for 5 min prior to the addition of small aliquots of a highly concentrated heparin solution (220 and/or 2200 μM) with minimal dilution (less than 5%), and the instantaneous decrease in fluorescence signal was read.

The dependence of the relative fluorescence change, i.e. $\Delta F/F_0 = (F_0 - F_{obs})/F_0$, where F_0 is the initial peptide solution fluorescence value and F_{obs} is the observed fluorescence value after each addition of heparin, was analysed by non-linear least-

squares data fitting by the binding equation (eqn 1), as described in [22], using Grafit Software ([32]; also see the website http://www.erithacus.com):

$$\frac{\Delta F}{F_0} = \frac{\Delta F_{max}}{F_0} \times \frac{[(P+nH+K_d) - \sqrt{(P+nH+K_d)^2 - 4 \cdot P \cdot nH}]}{2P} \quad (1)$$

where P is the total peptide concentration, H represents the added heparin concentration, n is the stoichiometry, K_d is the dissociation constant and $\Delta F_{max}/F_0$ is the maximum relative fluorescence change. The same effect is obtained if a fixed concentration of heparin is titrated with small aliquots of a highly concentrated solution of peptide; however, the inflection of the curve is in the opposite direction. The stoichiometry of the interaction was calculated by using the Hill plot, i.e. the slope of $\log(\Delta F/F_0) \times \log[H]$, considering only the linear part of the curve (generally that encompassing 15 and 85 % of the maximum effect [33]) on the basis of the following eqns:

$$P + nH \leftrightarrow nPH \quad (2)$$

$$K_{app} = \frac{[P] \cdot [H]^n}{[nPH]} \quad (3)$$

and $\Delta F_{max} = [P]_{total}$, corresponding to 100 % saturation, and $\Delta F = [nPH]$, corresponding to partial saturation. Rearranging eqns (1) and (2) yields eqns (4) and (5):

$$\frac{\Delta F}{\Delta F_{max}} = \frac{[(P+nH+K_d) - \sqrt{(P+nH+K_d)^2 - 4 \cdot P \cdot nH}]}{2P} \quad (4)$$

$$\frac{[H]^n}{K_{app} + [H]^n} = \frac{[nPH]}{[P]} \quad (5)$$

Combining eqns (4) and (5) gives rise to the following equation:

$$\frac{[H]^n}{K_{app} + [H]^n} = \frac{[nPH]}{[P]} = \frac{\Delta F}{\Delta F_{max}} = \frac{[(P+nH+K_d) - \sqrt{(P+nH+K_d)^2 - 4 \cdot P \cdot nH}]}{2P}$$

which are the two forms of describing the phenomenon, the first part stands for the equilibrium, whereas the second represents the ligand depletion. Applying logs to both sides of the equation and rearranging it, gives rise to linearization and provides a means to calculate the stoichiometry according to the Hill plot:

$$\log \frac{\Delta F}{F_0} = n \cdot \log[H] - \log K_{app} \quad (6)$$

The effect of the ionic strength on the dissociation constant was investigated by adjusting the buffer ionic strength with NaCl. The K_d value relates to the ionic strength according to the polyelectrolyte theory of Record et al. [34] by using eqn (7):

$$\log K_d = \log K_{NI} + Z\psi \log I \quad (7)$$

where K_{NI} is the non-ionic dissociation constant at 1 M NaCl, Z is the number of ionic interactions, I is the ionic strength and ψ is the fraction of bound counter-ion for each charged site on the polysaccharide that is released upon binding to the peptides.

The ionic strength of the buffer solution was calculated according to eqn (8):

$$I = 0.5 \cdot (C_1 \cdot Z_1^2 + C_2 \cdot Z_2^2 + \cdots + C_n \cdot Z_n^2) \quad (8)$$

where I is the ionic strength; C is the molar concentration and Z is the charge.

CD spectrometry

CD measurements in far-ultraviolet regions (195–260 nm) were performed in a JASCO J-700 spectropolarimeter scanning at a rate of 100 nm/min at 37 °C. Cells of 0.1 cm for the far-UV experiments were used. The experiments were performed in 10 mM Tris/HCl, pH 7.4, containing 50 μM of each peptide. The observed ellipticity was normalized to units of degrees.cm^2.dmol^{-1}. All dichroic spectra were smoothed and corrected by subtraction of the background for the spectrum obtained either with buffer alone or buffer containing heparin. The CD spectra for the peptides were analysed for the relative amounts, in percentage terms, of the secondary structural elements using a program based on comparison with the spectra obtained for the structures of known proteins. The results were also compared with the fractional percentage α-helix content calculated from $[\theta]_{222\ nm}$ as described by Chakrabartty et al. [35], and Sreerama and Wood analysis [36].

Time-resolved fluorescence

Time-resolved experiments were performed using an apparatus on the basis of the time-correlated single-photon-counting method. The excitation source was a Tsunami 3950 Spectra Physics titanium–sapphire laser, pumped by a 2060 Spectra Physics argon laser. The repetition rate of the 5 ps pulses was set to 400 kHz or 800 kHz using the pulse picker 3980 Spectra Physics. The laser was tuned to give output at 930 nm and a third harmonic generator BBO crystal (GWN-23PL Spectra Physics) gave the 310 nm excitation pulses that were directed to an Edinburgh FL900 spectrometer, where the emission wavelength was selected by a monochromator, and emitted photons were detected by a refrigerated Hamamatsu R3809U micro-channel plate photomultiplier. The L-format configuration of the spectrometer allowed the detection of the emission at right angles from the excitation source, and for anisotropy measurements a Glan Thompson polarizer in the emission beam and a Soleil Babinet compensator in the excitation beam were employed respectively. The FWHM ('full width at half-maximum') of the instrument response function was typically 45 ps, determined with a time resolution of 6.0 ps per channel. Measurements of the peptide decays were made using a time resolution of 12 ps per channel or 24 ps per channel, depending on the presence of the acceptor. Software provided by Edinburgh Instruments was used to analyse the decay curves, and the adequacy of the multi-exponential decay fitting was judged by inspection of the plots of weighted residuals and by statistical parameters, such as the reduced chi-square method.

Computation

The fluorescence decay of the donor, characterized by its lifetime τ_d, becomes faster in the presence of the acceptor bound to the peptide. Eqn (9) describes the intensity decay in the case of a fixed distance between donor and acceptor groups:

$$I(t) = I_0 \exp\left[\left(-\frac{1}{\tau_d} - \frac{R_o^6}{\tau_d r^6} \right) t \right] \quad (9)$$

However, this equation fails to fit to the experimental decay when more than one distance is present during the time decay of the fluorophore. If the distance distribution can be represented by a function $f(r)$, it can be recovered from the experimental data by using the CONTIN program [37], which inverts general

Table 1 IQF peptides with a Cardin motif and dissociation constant (K_d) with the stoichiometry (n) for their interaction with low-molecular-mass heparin

Conditions for K_d determination used were 50 mM Tris/HCl, pH 7.4/100 mM NaCl/0.2% (w/v) PEG 6000 at 37 °C. N. I., no interaction was detected with heparin; N. D., not determined.

Name	Sequence of peptide	K_d* (nM)	Stoichiometry† (n)
KK-1	Abz-A-K-K-A-R-A-Q-EDDnp	N. I.	–
KK-2	Abz-A-K-K-A-R-A-A-K-K-A-R-A-Q-EDDnp	2690 ± 80	0.5
KK-3	Abz-A-K-K-A-R-A-A-K-K-A-R-A-A-K-K-A-R-A-Q-EDDnp	153 ± 15	1.0
KK-4	Abz-A-K-K-A-R-A-A-K-K-A-R-A-A-K-K-A-R-A-A-K-K-A-R-A-Q-EDDnp	82 ± 5	0.9
RKK-1	Abz-A-R-K-K-A-A-K-A-Q-EDDnp	N. I.	–
RKK-2	Abz-A-R-K-K-A-A-K-A-A-R-K-K-A-A-K-A-Q-EDDnp	1103 ± 20	0.7
RKK-3	Abz-A-R-K-K-A-A-K-A-A-R-K-K-A-A-K-A-A-R-K-K-A-A-K-A-Q-EDDnp	21 ± 4	1.1
RKK-4	Abz-A-R-K-K-A-A-K-A-A-R-K-K-A-A-K-A-A-R-K-K-A-A-K-A-A-R-K-K-A-A-K-A-Q-EDDnp	8 ± 1	0.9
KK-A	Abz-A-K-K-A-R-A-A-K-K-A-R-A-A-K-K-A-R-A-Q-NH_2	N. D.	–
KK-Q	A-K-K-A-R-A-A-K-K-A-R-A-A-K-K-A-R-A-Q-EDDnp	N. D.	–

* The K_d value is already corrected as a function of the stoichiometry, i.e. $(K_d)^n$.
† n is the stoichiometry calculated according to the Hill plot.

systems of linear algebraic equations of the type:

$$y(t_k) = \int_a^b f(r)K(r,t_k)\,\mathrm{d}r + \sum_{j=1}^{N_L} L_{kj}\beta_i, \quad k = 1,\ldots N_y \tag{10}$$

In our experimental conditions, $y(t_k)$ corresponds to the observed intensity of fluorescence at the instant t_k. The distance distribution function $f(r)$ is recovered within a chosen interval for r, initially set between 5 to 100 Å (1 Å ≡ 0.1 nm), divided in N equally spaced intervals, and the integral is converted, by numerical integration, into a summation in r_j. The function inside the integral is then written as $K(r_j, t_k)$ and corresponds to eqn (10), written for the instant t_k and deconvoluted from the instrument response function, and assumed to be valid for each distance r_j within the chosen interval. The second term in eqn (10) accounts for 'impurities' that may be present contributing to the decay profile. The program recovers the parameter β_j corresponding to the contribution L_{kj} of the jth impurity to the fluorescence intensity at the instant t_k. In the analysis we also imposed the constraint of non-negativity for the distribution function. The best solution was found using the weighted least-squares method with the employment of a regularizer on the basis of the principles of parsimony [37].

The distance R_o, as used in eqn (11) for the function $K(r_j, t_k)$, was determined from the spectral data of the donor's emission $F_d(\lambda)$ and acceptor's molar absorption coefficient for absorption $\epsilon_a(\lambda)$, i.e.

$$R_o^6 = \frac{9000(\ln 10)\kappa^2\Phi_d}{128\pi^5 n^4 N_0}\int F_d(\lambda)\epsilon_a(\lambda)\lambda^4\,\mathrm{d}\lambda \tag{11}$$

where n is the refractive index of the medium, Φ_d is the quantum yield of the donor and κ is the orientation term dependent on the relative angles between dipoles' moments from donor and acceptor.

RESULTS

Synthesized peptides

Table 1 shows the IQF peptides synthesized on the basis of Cardin motifs [29] that were previously reported by Verrecchio et al. [21] for heparin binding. The peptides were divided into two series based upon the kernel of the heparin-binding motif (KK or RKK). Tandem repeats (up to 4-mer) of each pattern were synthesized, and the peptides were named after the pattern and the number of repeats. Two peptides derived from peptide KK-3 were synthesized as controls, one containing only the fluorescent probe (KK-A) and the other containing only the quencher group (KK-Q). Table 2 shows the sequence of IQF peptides synthesized based upon part of the reported heparin-binding sites of antithrombin-III (AT3D) [6] and kallistatin (HC2) [8]. Antithrombin-III Cys^{128} residue, originally included in this segment, which is disulphide-bounded to Cys^{8}, was replaced by a methionine residue. For comparison, we have synthesized two other peptides derived from kallistatin that also contain basic residue clusters (HC1 and HF). The IQF peptides related to the reactive-centre loops of kallistatin (KLL) and α_1-antichymotrypsin (ACT) were also studied, because their hydrolysis by human tissue kallikrein and cathepsin G, respectively, was protected in the presence of heparin (results not shown). The peptides were named on the basis of the protein regions they derived, i.e. for kallistatin, KLL corresponds to its reactive centre loop; HC1 is from the region between the H helix and the C1 sheet; HC2 is from H helix and C2 sheet; HF is from helix F. For antithrombin III, AT3D is derived essentially from the D helix, which was demonstrated to be part of the heparin-binding site in the three-dimensional structure of the antithrombin III–heparin complex crystal [5,6,38].

Heparin alters the fluorescence of the IQF peptides

Figure 2 shows the effect of the addition of highly concentrated aliquots of heparin solution (220 μM and/or 2200 μM, with final dilution less than 5%) over a buffered 1.05 μM RKK-2 peptide solution. Initially, the peptide fluorescence decreases steeply by the addition of heparin, followed by a slower decrease till the saturation is reached after approx. 1 μM heparin concentration, and no further change in the fluorescence is observed. The fluorescence remained in the saturated IQF peptide–heparin complexes, indicating that the complexes are partially quenched. The inset of Figure 2 shows the same interaction, but through the addition of a highly concentrated peptide solution over a buffered heparin solution. The lower slope represents heparin titration and, after the inflexion point that is the end of titration, the upper slope corresponds to a variation in the fluorescence as if only peptide was added. The stoichiometry obtained by simple inspection of these graphics is between 0.4 and 0.7, and since this method is very approximate and has a high level of error, it is not significantly different to the value of 0.7 (RKK-2; Table 1) obtained from the Hill plot. Moreover, the fluorescence of 0.3 μM peptide KK-A solution, which contains only the fluorescent group, did not change with progressive addition of

Table 2 IQF peptides derived from kallistatin, antithrombin III and α_1-antichymotrypsin, and dissociation constant (K_d) with the stoichiometry (n) for their interaction with low-molecular-mass heparin

Name	Serpin*	Sequence of peptide	K_d† (nM)	n‡
		Heparin-binding sites		
HC2	Kallistatin$^{300–319}$	Abz-R-W-N-N-L-L-R-K-R-N-F-Y-K-K-L-E-L-H-L-P-Q-EDDnp	17 ± 2	0.8
HC1	Kallistatin$^{107–126}$	Abz-F-N-L-T-E-L-S-E-S-D-V-H-R-G-F-Q-H-L-L-H-Q-EDDnp	79 000 ± 5000	0.2
HF	Kallistatin$^{176–195}$	Abz-V-G-T-I-Q-L-I-N-D-H-V-K-K-E-T-R-G-K-I-V-Q-EDDnp	27 0000 ± 10 000	0.2
AT3D	Antithrombin$^{112–139}$	Abz-S-E-K-T-S-D-Q-I-H-F-F-F-A-K-L-N-M-R-L-Y-R-K-A-N-K-S-S-K-Q-EDDnp	100 ± 6	0.8
		Reactive centre loop		
KLL	Kallistatin$^{384–401}$	Abz-A-I-K-F-F-S-A-Q-T-N-R-H-I-L-R-F-N-R-Q-EDDnp	712 ± 50§	1.0
ACT	Antichymotrypsin$^{379–397}$	Abz-K-I-T-L-L-S-A-L-V-E-T-R-T-I-V-R-F-N-R-Q-EDDnp	498 ± 11‖	0.8

* Numbering is on the basis of the SwissProt entries. Conditions used for K_d determination were 50 mM Tris/HCl, pH 7.4/100 mM NaCl/0.2% (w/v) PEG 6000, 37 °C.
† The K_d value is already corrected as a function of the stoichiometry, i.e. $(K_d)^n$.
‡ n is the stoichiometry calculated according to the Hill plot.
§ Buffer used was 20 mM Tris/HCl, pH 9/1 mM EDTA at 37 °C.
‖ Buffer used was 50 mM Tris/HCl, pH 8/5 mM $CaCl_2$ at 37 °C.

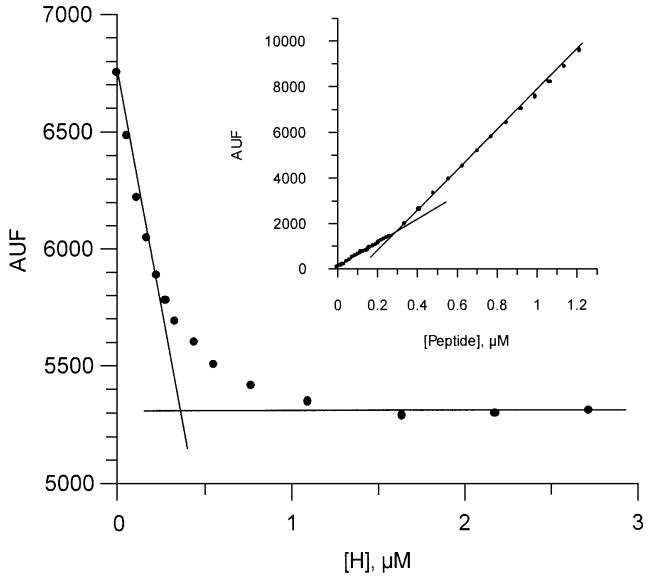

Figure 2 Fluroescence of RRK-2 peptide in the presence of 4500 Da heparin

RKK-2 peptide (1.05 μM; see Table 1) has its fluorescence diminished by the addition of increasing concentrations of 4500 Da heparin in 50 mM Tris/HCl, pH 7.4 containing 100 mM NaCl and 0.2% (w/v) PEG 6000 at 37 °C. The two lines represent the two phases of this titration, the end-point being significantly different from the blank. The inset shows an alternative experiment: 0.2 μM 4500 Da heparin was titrated with increasing concentrations of RKK-2 peptide in 50 mM Tris/HCl, pH 7.4, containing 100 mM NaCl, 0.2% (w/v) PEG 6000 at 37 °C. The two phases are also present, the slope of the second curve being the same as if peptide was added to a buffered solution without heparin. AUF, arbitrary units of fluorescence.

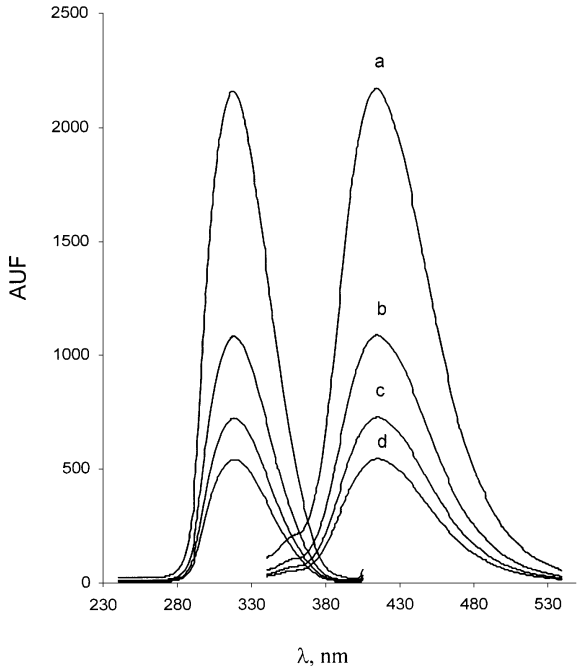

Figure 3 Juxtaposed excitation and emission spectra of RKK-2 peptide

Juxtaposed excitation (at λ_{ex} = 320 nm) and emission (at λ_{em} = 420 nm) spectra of RKK-2 peptide (1.05 μM; Table 1) are shown at heparin concentrations of 0 nM (trace a), 100 nM (trace b), 200 nM (trace c) and 300 nM (trace d) in 50 mM Tris/HCl containing 100 mM NaCl, 0.2% (w/v) PEG 6000, pH 7.4, 37 °C. The effect of heparin addition is observed both at excitation and emission spectra and no blue or red shifts were detected.

heparin up to 30 μM. Similarly, the fluorescence of an equimolar solution of peptides KK-A and KK-Q (1.2 μM each) also did not change up to the addition of 50 μM heparin, although heparin was able to complex with each one of these peptides, as revealed in the CD spectra (results not shown). These observations indicate that heparin does not promote unspecific aggregation of these peptides.

A solution of heparin–peptide complex was stored at room temperature for a period of 10 h, and its HPLC did not show any difference in the retention time or in the area of the peak of the peptide when compared with the initial peptide solution. The MALDI-TOF spectrometric mass analysis of the same solution also indicated the integrity of the peptide (results not shown). The absorbance wavelength scan of IQF peptides spanning the range 200–800 nm did not show any shift in the presence or in the absence of heparin (results not shown). Figure 3, on the other hand, shows the effect of heparin on the excitation and emission spectra of peptide RKK-2. The spectra were collected in the absence (trace a) and in the presence (traces b, c and d) of different concentrations of heparin, and the effects were observed solely on the intensity of the maximum for both the excitation and the emission, and no red or blue shift was detected.

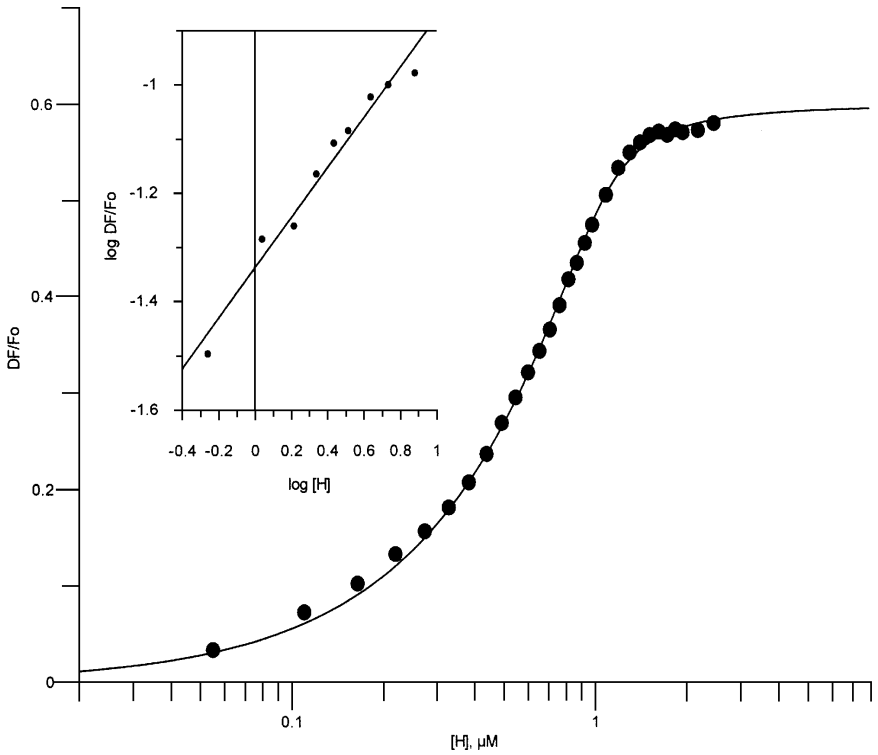

Figure 4 Semi-logarithmic plot of the non-linear fit of the effect of the addition of heparin on RKK-2 peptide

Semi-logarithmic plot of the non-linear fit [according to eqn (1)] of the effect of the addition of heparin on RKK-2 peptide (1.21 μM; Table 1) in 50 mM Tris/HCl, pH 7.4, containing 100 mM NaCl and 0.2% (w/v) PEG 6000 at 37 °C. The inset shows a Hill plot for this interaction, utilizing the data points featured between 15 and 85% of the maximum effect. The slope for this line is the stoichiometry for the interaction (h).

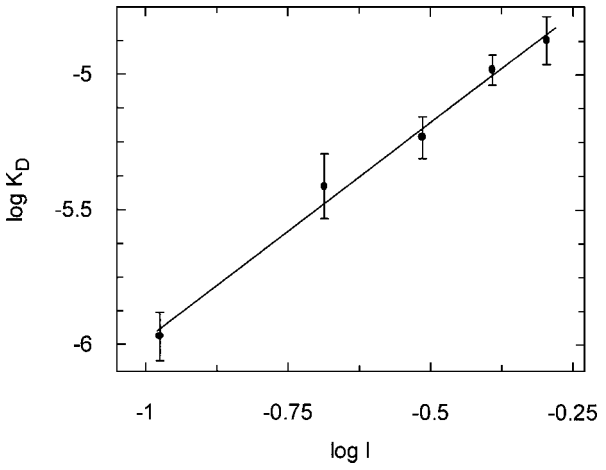

Figure 5 Ionic strength effect on the binding of IQF peptides to heparin

The fluorescence of RKK-2 peptide (0.2 μM; Table 1) was monitored while titrating with 50 mM Tris/HCl, pH 7.4, containing NaCl at concentrations of 100, 200, 300, 400 and 500 mM. These data were fitted to eqn (7) and provided a slope of 1.60 ± 0.08 and an intercept of -4.37 ± 0.05, yielding $K_{NI} = 42.6$ μM and $Z = 2.0$. The data are shown as mean values $\pm$ S. D. for each K_d calculation, shown by the error bars above and below each point.

K_d determination for heparin binding to peptides

Figure 4 shows the semi-logarithmic plot of $\Delta F/F_0$ against heparin concentration for the interaction of 1.21 μM RKK-2 with heparin according to eqn (1), and the inset shows the Hill plot for the same data. These are representative curves of all fluorescent titrations performed in this work. The obtained K_d values for the interaction of the KK and RKK Cardin motif peptides with heparin are shown in Table 1. The shorter KK-1 and RKK-1 peptides did not bind to heparin, but as the size of the peptides increased, the K_d values decreased, indicating that the affinity of the peptides for heparin is dependent on their sizes and on the number of positive charges distributed along the sequences.

Table 2 shows the calculated K_d values for the peptides derived from kallistatin, antithrombin-III and α_1-antichymotrypsin. These data show that, although the peptides derived from the reactive centre loop are able to bind to heparin, their affinities for heparin are significantly lower than those obtained for the peptides derived from the binding sites in kallistatin and antithrombin-III. This was mainly observed for peptides HC-2 and AT3D, corresponding to the high-affinity heparin-binding sites on kallistatin and antithrombin-III respectively.

The stoichiometry values for the interaction of each peptide with heparin were obtained by Hill plot analysis, as shown in Figure 4, and shown in Table 1 and 2. The peptides with Cardin motif (Table 1) that have higher affinity for heparin (low K_d values) also presented a stoichiometry value near to 1. The observation above that the fluorescence of an equimolar solution of peptides KK-A and KK-Q (1.2 μM each), which contain only the fluorescent or quencher group, did not change up to the addition of 50 μM of heparin is in accordance with the stoichiometry ($n = 1$) obtained for the peptide KK-3, which contains a similar amino acid sequence, added with both Abz and EDDnp.

Table 3 Internally quenched fluorescent peptides with Cardin motif and dissociation constant (K_d) with the stoichiometry (n) for their interaction with the pentassaccharide AGA*IA$_M$

Conditions used for K_d determination were: 50 mM Tris/HCl, pH 7.4, containing 100 mM NaCl and 0.2% (w/v) PEG 6000 at 37 °C.

Name	Sequence of peptide	K_d* (nM)	n†
RKK-2	Abz-A-R-K-K-A-A-K-A-A-R-K-K-A-A-K-A-Q-EDDnp	9768 ± 120	1.4
RKK-4	Abz-A-R-K-K-A-A-K-A-A-R-K-K-A-A-K-A-A-R-K-K-A-A-K-A-A-R-K-K-A-A-K-A-Q-EDDnp	732 ± 20	0.6
AT3D	Abz-S-E-K-T-S-D-Q-I-H-F-F-F-A-K-L-N-M-R-L-Y-R-K-A-N-K-S-S-K-Q-EDDnp	9163 ± 506	0.3

* The K_d value is already corrected as a function of the stoichiometry, i.e. $(K_d)^n$.
† n is the stoichiometry calculated according to the Hill plot.

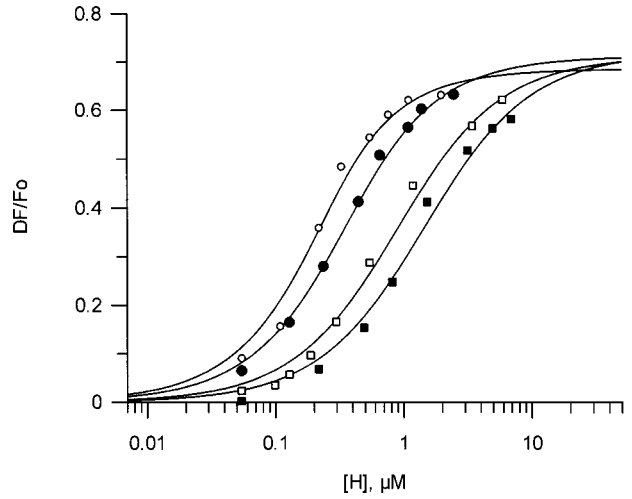

Figure 6 Semi-logarithmic plot of the non-linear fit, according to eqn (1), of the effect of the addition of heparin over 0.2 μm AT3D peptide, in the absence (open circles) or presence of 1.15 μg/ml (closed circles), 5.75 μg/ml (open squares) or 11.5 μg/ml (closed squares) protamine

Experiments were performed in 50 mM Tris/HCl, pH 7.4, containing 100 mM NaCl and 0.2% (w/v) PEG 6000 at 37 °C.

Table 4 α-Helix content determined by far UV-CD spectra (195–260 nm) of representative IQF peptides in the presence or absence of low-molecular-mass heparin

Conditions used were: 50 μM peptide in 10 mM Tris buffer, pH 7.4, at 37 °C in absence (buffer) and presence of 50 μM heparin. The evaluations of α-helical content were performed as described by the analysis of Sreerama and Woody [36] and by residue molar ellipticity at 222 nm (shown by values in parentheses). The error for these determinations was approx. 2%.

	α-Helical content (%)	
Peptide (source of peptide)	Buffer	Heparin
HC2 (kallistatin)	31.5 (26.5)	39.0 (35.5)
HF (kallistatin)	24.8 (28.0)	25.6 (56.4)
AT3D (antithrombin)	8.5 (8.6)	23.5 (24.3)
RKK-1 (Cardin-motif peptides)	Random coil	Random coil
RKK-4 (Cardin-motif peptides)	Random coil	89.6 (81.5)
KK-4 (Cardin-motif peptides)	Random coil	30.6 (25)

On the other hand, the shorter peptides KK-2 and RKK-2, which showed low affinity for heparin compared with the larger peptides (KK-3, KK-4, RKK-3 and RKK-4), had their stoichiometries of binding around 0.5.

The peptides derived from kallistatin, antithrombin III and α_1-antichymotrypsin (Table 2) showed the same overall correlation between stoichiometry and dissociation constants as for the peptides with the Cardin motif. Stoichiometry values near to 1 were observed for peptide HC2, which corresponds to the more probable heparin-binding site in kallistatin, and peptide AT3D, which is part of the heparin-binding site in antithrombin III. The peptides containing the reactive centre loops of kallistatin and α_1-antichymotrypsin also have stoichiometry values close to 1, despite their high K_d values. On the other hand, the kallistatin-derived peptides HC1 and HF showed low affinity and heparin–peptide stoichiometries of 0.2.

The variation in the dissociation constant over the ionic strength of the buffer for the binding of peptide RKK-2 is shown in Figure 5 by plotting the linear fit of the logarithm of the dissociation constants against the log of the ionic strength. According to the polyelectrolyte theory of Manning and Record (eqn 7), the y-axis intercept is the log of the dissociation constant at 1 M salt and represents the strength of the non-ionic binding (K_{NI}), and the slope is related to the number of ionic interactions (Z) by the fraction of univalent counter-ions released upon binding to the peptide (ψ), taken as 0.8 for heparin [19]. For this peptide, the obtained slope was 1.62 ± 0.12 and the y-axis intercept was -4.57 ± 0.07, yielding $Z = 2.00$ and $K_{NI} = 42.6\ \mu$M respectively.

Figure 6 shows the effect of protamine on the binding of IQF peptide to heparin. On increasing the amount of protamine, the titration curve of AT3D peptide with heparin is displaced to the right, indicating competition for heparin between the IQF peptide and protamine.

We also examined the interaction of the synthetic pentasaccharide AGA*IA$_M$ with the IQF peptides RKK-2, RKK-4 and AT3D. Table 3 shows the obtained K_d values. In comparison with the values with 4500 Da heparin (Table 1 and 2), the K_d for RKK-2 with the pentasaccharide was one order of magnitude higher, and the K_d for the IQF peptides RKK-4 and AT3D were two orders of magnitude higher. The stoichiometry for these two peptides with the pentasaccharide is lower than that obtained with 4500 Da heparin. Another significant difference between the interactions of these polysaccharides with the three examined IQF peptides was the lower values for the maximum decrease in fluorescence observed with the pentasaccharide (10–15% of initial fluorescence) in comparison with 4500 Da heparin (20–40% of initial fluorescence). These differences in the fluorescence decrease with IQF peptides upon binding to 4500 Da heparin and pentasaccharide is a result of the conformation adopted by each peptide, and also by the different stoichiometry of the interaction.

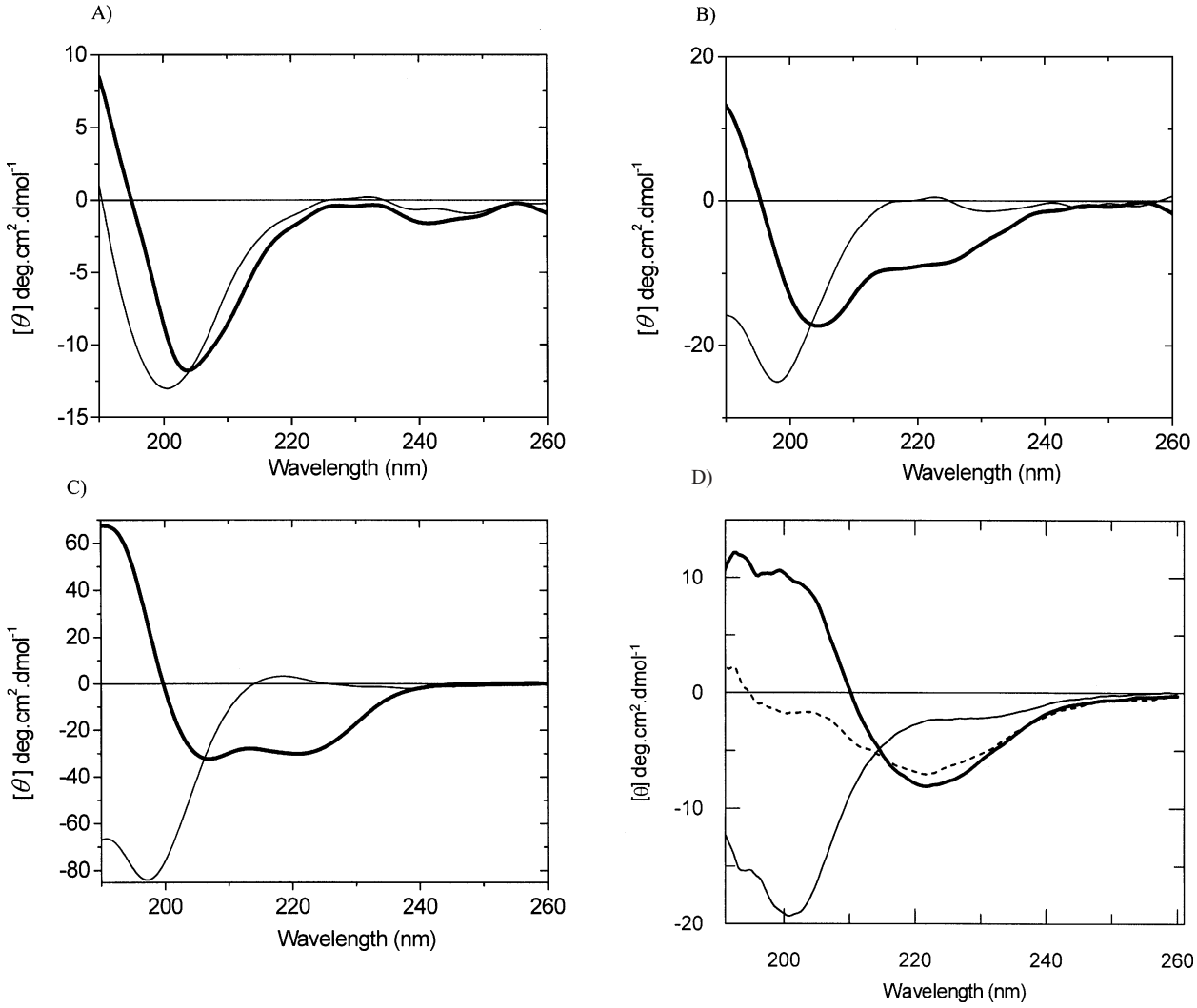

Figure 7 CD spectra of representative peptides

Peptides studied were (**A**) peptide KK-1 (Abz-A-K-K-A-R-A-Q-EDDnp), (**B**) peptide KK-4 (Abz-A-K-K-A-R-A-A-K-K-A-R-A-A-K-K-A-R-A-A-K-K-A-R-A-Q-EDDnp) and (**C**) peptide RKK-4 (Abz-A-R-K-K-A-A-K-A-A-R-K-K-A-A-K-A-A-R-K-K-A-A-K-A-A-R-K-K-A-A-K-A-Q-EDDnp) (amino acids are shown using the single-letter code). The thinner lines in (**A**–**C**) are the spectra pertaining to the 50 μM peptides collected in 10 mM Tris-HCl, pH 7.4, in the absence of heparin, and the thicker lines represent the spectra collected after the addition of 50 μM 4500 Da heparin. Corrections were made for the buffer and added heparin. (**D**) CD spectra of AT3D, a peptide derived from the D helix of human anti-(thrombin-II). Thin line, 50 μM AT3D; thick line, 50 μM AT3D with 50 μM 4500 Da heparin added; dotted line, 50 μAT3D with pentasaccharide AGA*IA$_M$ (50 μM) added. Experiments were performed in 10 mM Tris/HCl, pH 7.4, at 37 °C.

CD spectra

The far-UV–visible CD spectra of the peptides KK-1, KK-4, RKK-4 and AT3D are shown in Figures 7(A), 7(B), 7(C) and 7(D) respectively. The fractional percentage of α-helix content calculated from $[\theta]_{222\ nm}$, as described by Chakrabartty et al. [35] and by Sreerama and Wood analysis [36], are shown in Table 4. Peptide AT3D exhibited approx. 8 % α-helix structure, and the addition of an equimolar quantity of 4500 Da heparin induced an increase in the α-helix content of peptide ATD3. For peptide HC2, the Sreerama and Woody analysis [36], as well as the residue molar ellipticity at 222 nm, indicate that the increase in α-helix content was not significant, although drastic spectral alterations were observed. These data suggest that heparin induces other types of secondary structures in which the end-to-end distances should be shorter than in the flexible random conformation, because the fluorescence of peptide HC2 decreases approx. 30 % in the presence of heparin. The Sreerama and Woody analysis [36], when compared with the residue molar ellipticity at 222 nm for the secondary structure of the peptide HF, does not correlate (Table 4), possibly because the peptide–heparin complex exhibits an atypical secondary structure.

The CD spectra of the peptides KK-1, KK-4 and RKK-4 (Figures 7A, 7B and 7C) clearly indicate the presence of a totally random structure, which was corroborated by the calculated residue molar ellipticity at 222 nm. Heparin induced a significant amount of α-helix on the peptides RKK-4 and KK-4 (Table 4), and the obtained values of α-helix content suggest that heparin induces the occurrence of eight turns of helix in the peptide RKK-4 (Figure 7C). Only visible-light spectral analysis was possible for the peptide KK-1 (Figure 7A), because this peptide has a sequence that prevents the formation of any type of secondary structure, and in this case, the CD spectrum suggests

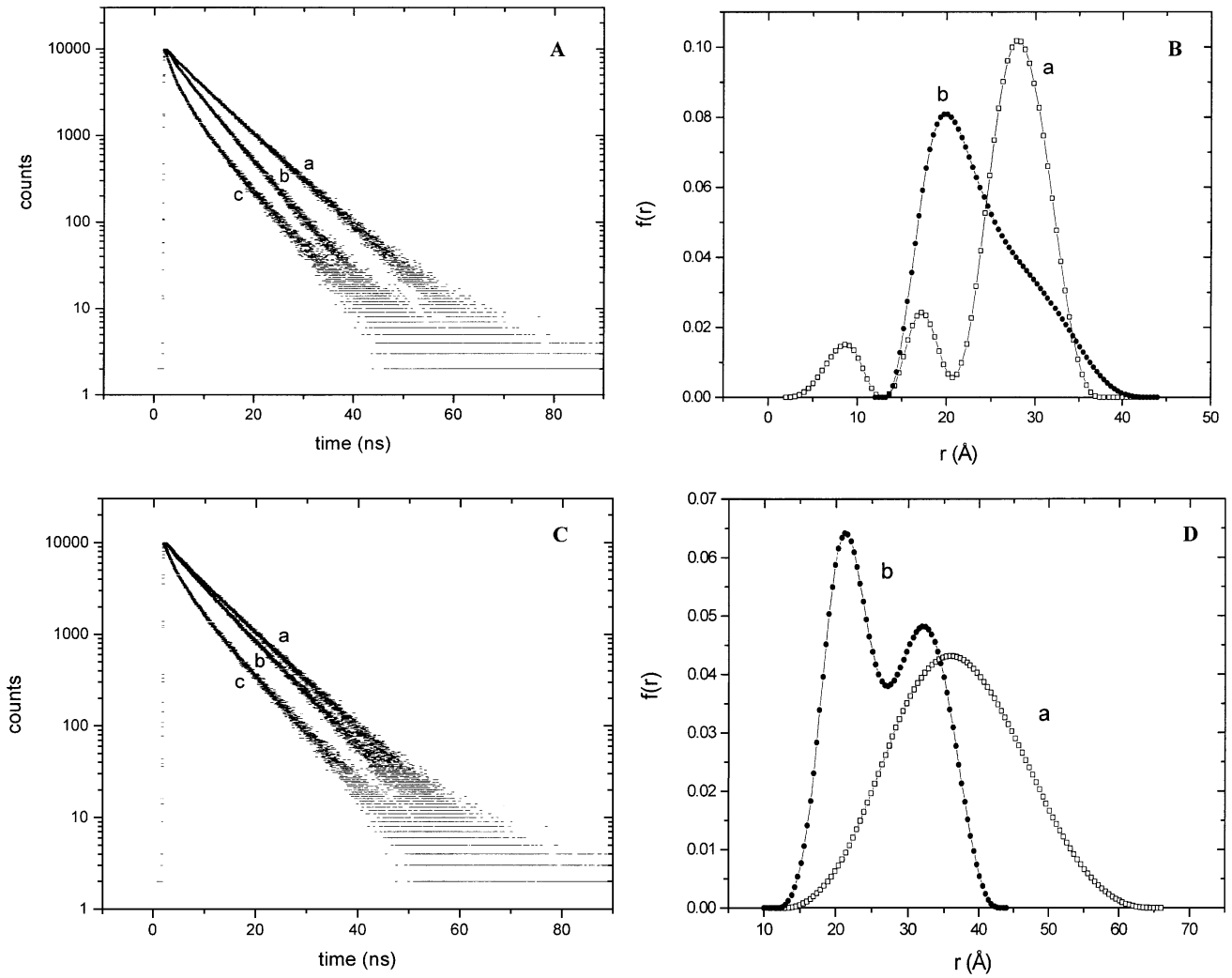

Figure 8 Fluorescence decay curves for peptides KK-A, KK-4 and RKK-4 in the presence of 30 μM heparin (a and c), and distance distribution for KK-4 (b) and RKK-4 (d) recovered using the CONTIN program

(**A**) Fluorescence decay curves in Hepes buffer 50 mM, pH 7.4, measured at 37 °C, with (trace a) 30 μM KK-A, (trace b) 30 μM KK-4 or (trace c) 30 μM KK-4 in the presence of 30 μM heparin. (**B**) Distance distribution for KK-4 recovered using the CONTIN program, for (trace a) 30 μM KK-4 in 50 mM Hepes buffer, pH 7.4, at 37 °C and in the presence of 30 μM heparin (trace b). (**C**) Fluorescence decay curves in 50 mM Hepes buffer, pH 7.4, measured at 37 °C. (Trace a) 30 μM KK-A; (trace b) 30 μM RKK-4; (trace c) 30 μM RKK-4, all in the presence of 30 μM heparin. (**D**) Distance distribution for RKK-4 recovered using the CONTIN program. (Trace a) 30 μM RKK-4 in 50 mM Hepes buffer, pH 7.4, at 37 °C, and in the presence of 30 μM heparin (trace b).

little organization of the peptide chain. Figure 7(D) shows the CD spectra of AT3D peptide both alone and in its complex with 4500 Da heparin and the synthetic pentasaccharide. The CD spectra are significantly different, and the content of α-helix is higher with the complex of 4500 Da heparin with AT3D (24% α-helix; Table 4) than with the complex with the pentasaccharide (16% α-helix)

Fluorescence decay

Table 5 shows that, in Hepes buffer, pH 7.4, the fluorescence decay of the peptide KK-A, which is labelled only with the Abz group (Figure 8A, curve a) is dominated by a lifetime of 8.2 ns, responsible for more than 80% of the total fluorescence emission. The decay is fitted best with the inclusion of a shorter lifetime of 3.25 ns, which accounts for 10% of the total fluorescence emission, and a fast component of 0.73 ns. A mean lifetime τ, calculated from a weighted average of the individual lifetimes and the corresponding normalized pre-exponential factors, is equal to 7.7 ns, comparable with that obtained for the labelled peptide Abz-bradykinin-NH_2 [28] and slightly below the value (8.1 ns) reported for the labelled amino acid Abz-Arg-NH_2 [39]. When heparin is present in the medium, at a peptide:heparin equimolar concentration (30 μM), the decay is best fitted to a three exponential function, with lifetimes 8.94, 5.03 and 0.75 ns and pre-exponential normalized factors equal to 0.60, 0.24 and 0.16 respectively, giving a mean lifetime value of 6.69 ns. An alternative procedure was to fit the experimental decay curves to lifetime distribution, and here also lifetime populations were obtained, centred in time values similar to those resulting from the multi-exponential fit. Mean lifetimes thus obtained were 7.67 ns for the peptide in Hepes and 6.45 ns when heparin was present in the medium.

The fluorescence of peptides labelled with both donor (Abz) and acceptor (EDDnp) groups decays faster due to the Förster resonance energy transfer from Abz to EDDnp, as shown in

Table 5 Time-resolved fluorescence parameters for the fluorescent peptide KK-A in buffer medium and in the presence of heparin

Conditions used were 30 μM KK-A in 50 mM Hepes buffer, pH 7.4 at 37 °C, in the absence or presence of 30 μM heparin. τ_i and a_i, lifetime and normalized pre-exponential factor for component i of the fluorescence decay; ϕ_i and b_i, rotational correlation time and normalized pre-exponential factor for component i of the anisotropy decay.

	Parameter									
	τ_1 (ns)	τ_2 (ns)	τ_3 (ns)	a_1	a_2	a_3	ϕ_1 (ns)	ϕ_2 (ns)	b_1	b_2
Buffer	8.24	3.25	0.73	0.81	0.022	0.023	0.069	0.412	0.106	0.252
Heparin	8.94	5.03	0.75	0.60	0.24	0.16	0.182	1.78	0.155	0.242

Figure 8 (A) (curve b) for the peptide KK-4. The increase in the decay rate was accentuated by the presence of heparin (Figure 8A, curve c), suggesting a decrease in the donor–acceptor distance due to the peptide–heparin interaction.

Estimation of Abz–EDDnp distance distribution

From the emission spectrum of the Abz-labelled peptide KK-A and the absorption spectrum of the C-terminal EDDnp-labelled peptide KK-Q, the overlap integral J and the Förster distance R_o were calculated. The calculation was similar to that described previously [28] for bradykinin labelled with the same donor and acceptor groups. Fast movement of both donor and acceptor groups was assumed during the excited state lifetime, so that the geometric parameter κ^2 was set equal to 2/3. This assumption was on the basis of measurements of time-resolved fluorescence anisotropy (Table 5). The anisotropy decay of Abz bound to the N-terminal of the peptide KK-A was best fitted to a bi-exponential decay. In buffer solution, without heparin, a shorter correlation time (0.069 ns) was observed and a longer (0.412 ns) component that changed to 0.182 ns and 1.78 ns, respectively, in the presence of heparin. Similar results were obtained for the peptide KK-4. The short correlation time is ascribed to the local motion of the fluorescent probe, indicating a fast rotational relaxation. The long component can be due to the overall tumbling of the peptide, and the interaction with heparin results in a complex of larger volume, decreasing the time rate of the anisotropy decay. The calculated Förster distance R_o in aqueous medium was equal to 24 Å, comparable with the value obtained in labeller bradykinins [28]. Spectroscopic data measured in the presence of heparin lead to a similar value for the distance R_o.

The decay profile of Abz emission in the peptides containing the acceptor group is complex and quite distinct from the decay curves of the peptides without EDDnp (Figure 8A). We analysed the experimental decay with the assumption that the distance between donor and acceptor is not fixed, as is usually found in peptides in aqueous medium. Then we used the CONTIN program to recover a distribution function $f(r)$ from the decay curve, without any *a priori* hypothesis concerning the distances r or the shape of the distribution curves. The results for the peptide KK-4, shown in Figure 8(B), reveal that most of the molecules (83 %) has an end-to-end distance of approx. 28 Å, and a minor population of the peptides presents shorter distances, near to 17 Å and below 10 Å. The longer peptide RKK-4 presents a broad distribution of end-to-end distance centred at approx. 36 Å, possibly reflecting structural flexibility of the peptide (Figure 8D).

When heparin is present in the medium, the end-to-end distance decreases, and the distance distribution for the peptide KK-4 shows a maximum in the population distance of approx. 19.7 Å, and a broad asymmetrical distribution extending to above 35 Å, revealing the presence of a population centred at approx. 30 Å partially superimposed on to the former distribution (Figure 8B). The peptide RKK-4, upon interaction with heparin, displays an equilibrium between two distance populations, centred at 32.9 and 21.2 Å, with relative contribution of 46 % and 54 % respectively (Figure 8D).

DISCUSSION

All the heparin-binding peptides labelled with the fluorescence donor and acceptor groups Abz and EDDnp at their N- and C-terminal ends respectively showed upon heparin binding a fluorescence decrease that was large enough to allow determination of K_d values up to 8 nM. The experimental procedures are as simple, fast and sensitive as those used to follow the fluorescence change of tryptophan in proteins that bind to heparin [22]. The calculated errors involved in the K_d determinations we obtained were similar to that reported for the interaction of heparin with antithrombin III, which involves the fluorescence of four tryptophan residues [40].

The K_d values for the binding of heparin to the shorter IQF peptides with the tandem repeats AKKARA and ARKKAAKA (Table 1) were lower than those previously reported with the same peptide sequences without Abz and Q (Gln)-EDDnp in a study that employed affinity co-electrophoresis [21] for the determination of K_d. The largest difference (24-fold) was observed when comparing the K_d values of peptides $(AKKARA)_2$ [21] and KK-2, which showed the lowest detectable affinity. This result suggests that Abz and/or Q-EDDnp might take part in the non-ionic heparin–peptide interaction, particularly in short peptides, because the ionic interactions with the peptide $(AKKARA)_2$ are less than those found in any other peptide, and the relative effects of Abz and Q-EDDnp on binding to heparin would be higher. According to this hypothesis, the value of $K_{NI} = 42.6\ \mu$M for the binding of heparin to peptide RKK-2 (Figure 5), which is the dissociation constant at 1 M salt concentration (representing the strength of the non-ionic binding), is very significant. Peptide RKK-4 has the strongest peptide–heparin interaction so far reported, as demonstrated by its K_d of 8 nM, which is approx. 3 times lower than the K_d reported for its homologue peptide $(ARKKAAKA)_4$ [21]. In this larger heparin-binding peptide, with high affinity for heparin, the effects of Abz and Q-EDDnp seemed to be absent, or, if present, they were quite small. The CD spectra of peptides KK-4 and RKK-4 indicated a significant induction of α-helix by heparin, which is in accordance with previous observations with the peptide $(AKKARA)_6$ [21]. Although the increase in the concentration of heparin above the 1:1 stoichiometry disrupted the α-helix detected by CD spectroscopy [21], no variation in the fluorescence of the peptide–heparin 1:1 complexes was observed after the addition of heparin up to a concentration that was 5 times higher than the peptide concentration. These observations suggest that the structure of the

peptide–heparin complex may be modified by the addition of extra heparin, but the end-to-end distance of the peptides in the complex does not change, at least not to an extent that could be detected by fluorescence measurements.

The amino acids Lys^{312}–Lys^{313} in the region between the H helix and C2 sheet of kallistatin comprise the major heparin-binding site responsible for kallistatin's heparin-suppressed human tissue-kallikrein binding [8]. The peptide HC2 encompasses the segment between the amino acids Arg^{300} to Pro^{319} of kallistatin, and its binding with heparin revealed a K_d value of 17 nM. Interestingly, this peptide contains two consensus heparin-binding motifs (XBBBXXB) between the residues Leu^{305} and Leu^{318}. On the other hand, peptide HC1 has only one consensus heparin-binding sequence in the segment His^{118}–His^{123}, and HF peptide has none. In addition, heparin–peptide stoichiometry for peptide HC2 was 1:1, whereas for the peptides HC1 and HF the stoichiometry was 0.2. Both of these peptides have significantly higher K_d values compared with that of peptide HC2. Although the region between the H helix and C2 sheet of kallistatin is the major heparin-binding site of this serpin [8], and peptide HC2, which encompasses this region, has a high affinity towards heparin, it cannot be concluded purely on an examination of the peptide–heparin interaction alone that this segment is the heparin-binding site in the whole protein. In fact, the low affinity of the pentasaccharide towards the peptide AT3D contrasts with the high affinity of this GAG for antithrombin III, in which the segment that the peptide AT3D encompasses is an important part of the pentasaccharide-binding site.

The CD spectra for the peptide HC2 did not show significant variation in the amount of α-helix upon heparin binding, although drastic spectral alterations were observed (results not shown). Moreover, in the kallistatin-modelled structure [41], the region corresponding to HC2 peptide is not in an α-helix conformation; therefore it is possible that the binding of heparin at this site, impairing the inhibition of human tissue kallikrein by kallistatin, occurs without any induction of α-helix.

Peptide AT3D, derived from antithrombin III segment Ser^{112}–Lys^{139}, has a significant affinity towards 4500 Da heparin (K_d 100 nM), which is of the same order of magnitude as the K_d values described for the interaction of antithrombin III with heparin [6,42,43]. The K_d value for the interaction of heparin with the peptide AT3D is approx. 1000-fold lower than that previously described for a shorter homologue peptide, acetyl-F^{123}AKLNCRLYRKANKSSK^{139} [23]. This observation suggests that the additional sequence S^{112}EKTSDQIHFF^{122} present in peptide AT3D plays a significant role in its binding to heparin. In contrast, the synthetic pentasaccharide AGA*IA_M showed a lower affinity for AT3D peptide, as was also observed with the peptides RKK-2 and RKK-4. The pre-existing α-helix of peptide AT3D in helix D of anti-thrombin III seems to be essential for the high-affinity binding of the pentasaccharide, and the small size of this pentasaccharide does not induce the convenient conformational change needed for its binding.

The fluorescence decay of labelled Cardin-motif peptides in aqueous solution is dominated by a lifetime component of approx. 8 ns, and the mean-lifetime value is comparable with those obtained for labelled amino acids or peptides [28,39]. In the presence of heparin, we detected an increase in the long-lifetime component, but its relative contribution decreases, resulting in a decreased mean lifetime. The anisotropy decay clearly demonstrates the formation of a peptide–heparin complex, as revealed by the increase in the long rotational correlation time when heparin was added in equimolar concentration to the peptide solution (Figure 8). That result is consistent with an increase in the volume associated with the rotational diffusion of the macromolecule to which the probe is attached, originating from the formation of a peptide–heparin complex.

Protamine toxicity justifies the search and development of alternative heparin-reversal compounds. Once heparin is in a mixture of polysaccharides, a polymer with masses distributed along a Gaussian curve, its activities over different proteins may depend on the chain length. Therefore the development of specific peptides to neutralize either all or part of heparin effects, which may lead to only one specific population of heparin molecules having its effect preserved, could be an important therapeutic strategy. In this way, IQF peptides containing Abz/Q-EDDnp as a donor/acceptor fluorescence pair provide a sensitive and handy method for evaluating the formation of peptide–heparin complexes, and to obtain structural information by means of an examination of the fluorescence decay in addition to their CD spectra analysis.

This work was supported by Fundação de Amparo Pesquisa do Estado de São Paulo (FAPESP), Conselho Nacional de Desenvolvimento Científico e Tecnológico (CNPq), and Human Frontiers for Science Progress (RG 00043/2000-M). We are grateful to Dr Adelaide Faljoni-Alario (Instituto de Química, Universidade de São Paulo) for collaboration in the CD analysis, and to Dr Otaciro Rangel Nascimento (Instituto de Física, Universidade de São Paulo) for the use of the JASCO J-700 spectropolarimeter. We are grateful to Dr S. W. Provencher for providing us with the CONTIN manual.

REFERENCES

1 Jackson, R. L., Busch, S. J. and Cardin, A. D. (1991) Glycosaminoglycans: molecular properties, protein interactions, and role in physiological processes. Physiol. Rev. **71**, 481–539
2 Lane, D. A., Denton, J., Flynn, A. M., Thunberg, L. and Lindahl, U. (1984) Anticoagulant activities of heparin oligosaccharides and their neutralization by platelet factor 4. Biochem. J. **218**, 725–732
3 Olson, S. T., Bjork, I., Sheffer, R., Craig, P. A., Shore, J. D. and Choay, J. (1992) Role of the antithrombin-binding pentasaccharide in heparin acceleration of antithrombin–proteinase reactions. Resolution of the antithrombin conformational change contribution to heparin rate enhancement. J. Biol. Chem. **267**, 12528–12538
4 Carrell, R. W., Evans, D. L. and Stein, P. E. (1991) Mobile reactive centre of serpins and the control of thrombosis. Nature (London) **353**, 576–578
5 Jin, L., Abrahams, J. P., Skinner, R., Petitou, M., Pike, R. N. and Carrell, R. W. (1997) The anticoagulant activation of antithrombin by heparin. Proc. Natl. Acad. Sci. U.S.A. **94**, 14683–14688
6 Belzar, K. J., Dafforn, T. R., Petitou, M., Carrell, R. W. and Huntington, J. A. (2000) The effect of a reducing-end extension on pentasaccharide binding by antithrombin. J. Biol. Chem. **275**, 8733–8741
7 Chuang, Y. J., Swanson, R., Raja, S. M. and Olson, S. T. (2001) Heparin enhances the specificity of antithrombin for thrombin and factor Xa independent of the reactive centre loop sequence. Evidence for an exosite determinant of factor Xa specificity in heparin-activated antithrombin. J. Biol. Chem. **276**, 14961–14971
8 Chen, V., Chao, L., Pimenta, D. C., Bledsoe, G., Juliano, L. and Chao, J. (2001) Identification of a major heparin-binding site in kallistatin. J. Biol. Chem. **276**, 1276–1284
9 Almeida, P. C., Nantes, I. L., Rizzi, C. C., Judice, W. A., Chagas, J. R., Juliano, L., Nader, H. B. and Tersariol, I. L. (1999) Cysteine proteinase activity regulation. A possible role of heparin and heparin-like glycosaminoglycans. J. Biol. Chem. **274**, 30433–30438
10 Almeida, P. C., Nantes, I. L., Chagas, J. R., Rizzi, C. C., Faljoni-Alario, A., Carmona, E., Juliano, L., Nader, H. B. and Tersariol, I. L. S. (2001) Cathepsin B activity regulation. Heparin-like glycosaminoglycans protect human cathepsin B from alkaline pH-induced inactivation. J. Biol. Chem. **276**, 944–951
11 Nielsen, P. and Yamada, Y. (2001) Identification of cell-binding sites on the Laminin α5 N-terminal domain by site-directed mutagenesis. J. Biol. Chem. **276**, 10906–10912
12 Nomizu, M., Kuratomi, Y., Malinda, K. M., Song, S. Y., Miyoshi, K., Otaka, A., Powell, S. K., Hoffman, M. P., Kleinman, H. K. and Yamada, Y. (1998) Cell binding sequences in mouse laminin α1 chain. J. Biol. Chem. **273**, 32491–32499
13 Spillmann, D., Witt, D. and Lindahl, U. (1998) Defining the interleukin-8-binding domain of heparan sulfate. J. Biol. Chem. **273**, 15487–15493
14 Kjellen, L. and Lindahl, U. (1991) Proteoglycans: structures and interactions. Annu. Rev. Biochem. **60**, 443–475
15 Tumova, S., Woods, A. and Couchman, J. R. (2000) Heparan sulfate proteoglycans on the cell surface: versatile coordinators of cellular functions. Int. J. Biochem. Cell Biol. **32**, 269–288

16 Deprez, P., Doss-Pepe, E., Brodsky, B. and Inestrosa, N. C. (2000) Heparan sulphate proteoglycans on the cell surface: versatile coordinators of cellular functions. Biochem. J. **350**, 283–290
17 Ferran, D. S., Sobel, M. and Harris, R. B. (1992) Design and synthesis of a helix heparin-binding peptide. Biochemistry **31**, 5010–5016
18 Jayaraman, G., Wu, C. W., Liu, Y. J., Chien, K. Y., Fang, J. C. and Lyu, P. C. (2000) Binding of a *de novo* designed peptide to specific glycosaminoglycans. FEBS Lett. **482**, 154–158
19 Olson, S. T. and Björk, I. (1991) Predominant contribution of surface approximation to the mechanism of heparin acceleration of the antithrombin–thrombin reaction. Elucidation from salt concentration effects. J. Biol. Chem. **266**, 6353–6364
20 Olson, S. T., Halvorson, H. R. and Björk, I. (1991) Quantitative characterization of the thrombin–heparin interaction. Discrimination between specific and non-specific binding models. J. Biol. Chem. **266**, 6342–6352
21 Verrecchio, A., Germann, M. W., Schick, B. P., Kung, B., Twardowski, T. and San Antonio, J. D. (2000) Design of peptides with high affinities for heparin and endothelial cell proteoglycans. J. Biol. Chem. **275**, 7701–7707
22 Olson, S. T., Björk, I. and Shore, J. D. (1993) Kinetic characterization of heparin-catalyzed and uncatalyzed inhibition of blood coagulation proteinases by antithrombin. Methods Enzymol. **222**, 525–559
23 Bae, J., Desai, U. R., Pervin, A., Caldwell, E. E. O., Weiler, J. M. and Linhardt, R. J. (1994) Interaction of heparin with synthetic antithrombin III peptide analogues. Biochem. J. **301**, 121–129
24 Schick, B. P., Gradowski, J. F., San Antonio, J. D. and Martinez, J. (2001) Novel design of peptides to reverse the anticoagulant activities of heparin and other glycosaminoglycans. Thromb. Haemost. **85**, 482–487
25 Chagas, J. R., Juliano, L. and Prado, E. S. (1991) Intramolecularly quenched fluorogenic tetrapeptide substrates for tissue and plasma kallikreins. Anal. Biochem. **192**, 419–425
26 Knight, G. C. (1995) Fluorimetric Assays of Proteolytic Enzymes. Methods Enzymol. **248**, 18–34
27 Gershkovich, A. A. and Kholodovych, V. V. (1996) Fluorogenic substrates for proteases based on intramolecular fluorescence energy transfer (IFETS). J. Biochem. Biophys. Methods **33**, 135–162
28 Souza, E. S., Hirata, I. Y, Juliano, L. and Ito, A. S. (2000) End-to-end distance distribution in bradykinin observed by Förster resonance energy transfer. Biochem. Biophys. Acta **1474**, 251–261
29 Cardin, A. D. and Weintraub, H. J. R. (1989) Molecular modeling of protein–glycosaminoglycan interactions. Arteriosclerosis **9**, 21–32
30 Ermolief, J., Boudier, C., Laine, A., Meyer, B. and Bieth, J. (1994) Heparin protects cathepsin G against inhibition by protein proteinase inhibitors. J. Biol. Chem. **269**, 29502–29508
31 Hirata, Y. I., Cezari, M. H. S., Nakaie, C. R., Boschcov, P., Ito, A. S., Juliano, M. A. and Juliano, L. (1994) Internally quenched fluorogenic protease substrates: solid-phase synthesis and fluorescence spectroscopy of peptides containing *ortho*-aminobenzoyl/dinitrophenyl groups as donor-acceptor pairs. Lett. Pept. Sci. **1**, 299–308
32 Leatherbarrow, R. J. (1992) Grafit Version 3.0, Erithacus Software Ltd, Staines, U.K.
33 Segel, I. H. (1993) Behavior and analysis of rapid equilibrium and steady-state enzyme systems. In Enzyme Kinetics, pp. 371–374, John Wiley and Sons, New York, NY
34 Record, M. T. J., Lohman, M. L. and De Haseth, P. (1976) Ion effects on ligand–nucleic acid interactions. J. Mol. Biol. **107**, 145–158
35 Chakrabartty, A., Schellman, J. A. and Baldwin, R. (1991) Large differences in the helix propensities of alanine and glycine. Nature (London) **351**, 586–588
36 Sreerama, N. and Woody, R. W. (1993) A self-consistent method for the analysis of protein secondary structure from circular dichroism. Anal. Biochem. **209**, 32–44
37 Provencher, S. W. (1982) A constrained regularization method for inverting data represented by linear algebraic or integral-equations. Comp. Physics Commun. **27**, 229–242
38 Ersdal-Badju, E., Lu, A., Zuo, Y., Picard, V. and Block, S. C. (1997) Identification of the antithrombin III heparin binding site. J. Biol. Chem. **272**, 19393–19400
39 Ito, A. S., Turchiello, R. F, Hirata, I. Y, Cezari, M. H. S., Meldal, M. and Juliano, L. (1998) Fluorescent properties of amino acids labeled with *ortho*-aminobenzoic acid. Biospectroscopy **4**, 395–402
40 Meagher, J. L., Beechem, J. M., Olson, S. T. and Gettins, P. G. (1998) Deconvolution of the fluorescence emission spectrum of human antithrombin and identification of the tryptophan residues that are responsive to heparin binding. J. Biol. Chem. **273**, 23283–23289
41 Chen, V., Chao, L. and Chao, J. (2000) A positively charged loop on the surface of kallistatin functions to enhance tissue kallikrein inhibition by acting as a secondary binding site for kallikrein. J. Biol. Chem. **275**, 40371–40377
42 Nordenman, B., Danielsson, A. and Bjork, I. (1978) The binding of low-affinity and high-affinity heparin to antithrombin. Fluorescence studies. Eur. J. Biochem. **90**, 1–6
43 Lindahl, U., Thunberg, L., Backstrom, G., Riesenfeld, J., Nordling, K. and Bjork, I. (1984) Extension and structural variability of the antithrombin-binding sequence in heparin. J. Biol. Chem. **259**, 12368–12376

Received 4 January 2002/2 May 2002; accepted 8 May 2002
Published as BJ Immediate Publication 8 May 2002, DOI 10.1042/BJ20020023